Adapted anisomorphic model for fatigue life prediction of CFRP laminates under constant amplitude loading

Broer, A.A.R.; Zarouchas, D.

DOI
10.1016/j.ijfatigue.2019.04.029

Publication date
2019

Document Version
Final published version

Published in
International Journal of Fatigue

International Journal of Fatigue 126 (2019) 270–283

Contents lists available at ScienceDirect

International Journal of Fatigue

journal homepage: www.elsevier.com/locate/ijfatigue

Adapted anisomorphic model for fatigue life prediction of CFRP laminates under constant amplitude loading

A.A.R. Broer, D. Zarouchas*

Structural Integrity & Composites Group, Faculty of Aerospace Engineering, Delft University of Technology, Kluyverweg 1, 2629HS Delft, Netherlands

ARTICLE INFO

Keywords:
Fatigue life prediction
Constant life diagram
Anisomorphic model

ABSTRACT

A new constant life diagram (CLD) model is proposed to predict the fatigue life of carbon fibre-reinforced epoxy laminates under constant amplitude (CA) loading. The CLD is asymmetric and non-linear, and it is built upon the anisomorphic CLD model. It consists of two sub-models; one sub-model is applicable to laminates with lay-ups characterised by a larger ultimate tensile strength (UTS) than absolute ultimate compressive strength (UCS): UTS $\geqslant$ |UCS|, while the second sub-model can be applied to those exhibiting the opposite tendency: |UCS| > UTS. Combined, the sub-models can predict the fatigue life of any carbon-epoxy laminate. The CLD can be constructed using only static strength data and fatigue life data related to one stress ratio (R), defined as either $R = 0.1$ or $R = -1.0$. An experimental campaign was conducted on a carbon-epoxy laminate with a lay-up of $[90/0/90]_{2S}$ to validate the first CLD sub-model. Additionally, a second case study from literature with a lay-up of $[45/90/\text{-}45/0]_{2S}$ was employed for validation. The second CLD sub-model was evaluated using two coupon case studies from literature with lay-ups of $[\pm 60]_{3S}$ and $[45]_{16}$. The predicted and experimentally obtained fatigue lives showed agreements for different R-ratios, and the observed prediction errors were in ranges similar to those of the original anisomorphic CLD model. Hence, the presented CLD model allows for fatigue life predictions in scales similar to experimental results while reducing the required experimental efforts with respect to the anisomorphic CLD model.

1. Introduction

Fibre-reinforced polymer (FRP) laminates are used in a variety of structures such as aircraft and wind turbines, in which they are continuously subjected to varying fatigue loads. These loads lead to deterioration of the material and ultimately to failure. It is important to determine the moment of failure based on its loading conditions, thereby allowing for potential maintenance actions. Moreover, knowledge of the fatigue life can be used as input to numerical models as shown by, for example, Passipoularidis et al. [18] and Samareh-Mousavi et al. [19]. A straightforward way to determine the time to failure is by conducting experimental tests under similar loading conditions as encountered in-service. However, fatigue testing is both time-intensive and costly, and an extensive test campaign is often not a viable solution. Therefore, it is necessary to develop fatigue life prediction methodologies that reduce the size of the experimental input dataset while ensuring reliable results.

Several approaches have been developed to predict the fatigue life of composites under constant amplitude (CA) loading. Most of these approaches can be associated with one of four categories: (1) empirically fitted stress-life (S-N) curves, (2) master S-N curves, (3) energy-based methods, or (4) constant life diagrams (CLDs). The empirically fitted S-N curves are the most straightforward, yet they require the most experimental data as input, since they interpolate between datapoints. Various relations between the applied stress and the fatigue life have been proposed such as the power-law and exponential formulations, as well as more elaborate functions; for example, Kohout and Věechet [14] extended the Basquin function to include a description of both the low- and high-cycle fatigue regions. Essentially, these models are descriptive functions of experimental data; when a different CA load cycle is considered, additional experimental tests are required. Contrarily, the master S-N curves reduce the size of the input dataset by adjusting an experimentally obtained S-N curve based on the loading conditions of interest. For example, Epaarachchi and Clausen [8] propose a modified slope based on the stress ratio (R-ratio), the loading frequency, and the fibre direction. The energy-based methods in the third category employ a fatigue failure criterion that relates the strain energy to the fatigue life. A relation is established using a dataset under one loading condition, which can then be used to predict the fatigue life under different R-ratios for different fibre directions. The application of

* Corresponding author.
E-mail address: D.Zarouchas@tudelft.nl (D. Zarouchas).

https://doi.org/10.1016/j.ijfatigue.2019.04.029
Received 11 February 2019; Received in revised form 18 April 2019; Accepted 23 April 2019
Available online 11 May 2019
0142-1123/

fatigue failure criterions to unidirectional off-axis composite laminates is shown by, amongst others, Ellyin and El-Kadi [7], Shokrieh and Taheri-Behrooz [21], and Varvani-Farahani et al. [24].

The approaches in the fourth category, the CLDs, are the focus of this work. The CLD is a predictive diagram that combines different S-N curves of all possible CA loads under similar environmental conditions. The ability to accurately construct such a diagram makes it possible to predict the S-N curve for any R-ratio. Several CLD shapes have been proposed in literature, not only the traditional Goodman and Gerber diagrams, but also more elaborated shapes by, for example, Boerstra [6], Gathercole et al. [9], Kawai and Koizumi [12], and Vassilopoulos et al. [26]. The latter models assess the asymmetry of the diagram for positive and negative mean stresses and assume a non-linear shape for the constant life lines (CLLs), resulting in more accurate predictions than the original Goodman and Gerber diagrams.

Ansell et al. [1] found that the CLLs peak in the vicinity of a specific R-ratio, the so-called critical R-ratio, which is the ratio between the ultimate compressive and tensile strength. Kawai and Koizumi [12] developed a new shape for the CLDs by combining Ansell's observation with the knowledge that CLLs for carbon FRP (CFRP) laminates can be described using a non-linear curve and that the diagram is asymmetric. In their model, the so-called anisomorphic model, the size of the input dataset is reduced with respect to other CLD models, which often employ several experimental S-N curves, because their CLD is constructed from a single experimental S-N curve. However, this S-N curve relates to the critical R-ratio, which is not conventionally used. Therefore, not much data for this R-ratio is found in literature, as can be seen in the OptiDAT [16] and the SNL/MSU/DOE database [15], which do not include fatigue life data for the critical R-ratio. Consequently, a direct implementation of the anisomorphic CLD model is often not possible. In most cases, even if fatigue life data is available, additional fatigue life experiments are required; alternatively, an approximation can be made by instead using test data under an R-ratio in the vicinity of the critical R-ratio. The latter is shown by Vassilopoulos et al. [25], who constructed the anisomorphic model for three laminates, and used data corresponding to $R = -1$ instead of $R = \chi = -0.76$, $R = -1$ data instead of $R = \chi = -0.77$ data, and $R = -0.5$ data instead of $R = -0.63$ data for the first, second, and third laminate, respectively. Furthermore, the anisomorphic CLD by Kawai and Koizumi [12] is invalid for certain angle-ply and off-axis unidirectional (UD) carbon-epoxy laminates, as shown by Kawai and Murata [13] and Kawai and Itoh [11], respectively. This led Kawai and Murata [13] and Kawai and Itoh [11] to develop the three- and four-segment anisomorphic CLD model that require two and three S-N curves as input, respectively, thereby counteracting initial advantages offered by the original (so-called two-segment) anisomorphic model of Kawai and Koizumi [12].

The goal of this study is to address the limitations of the anisomorphic model of Kawai and his colleagues by adapting the CLD model. Firstly, the critical R-ratio required as input is replaced with a more common R-ratio. Secondly, its aim is to use only a single experimental S-N curve as input rather than multiple S-N curves, as currently required for certain lay-ups. Both adaptations are made while keeping a similar predictive accuracy as in the anisomorpic models. In such a manner, the CLD can be applied more easily, and a reduction in the number of datapoints can be obtained. The model presented in this work employs only one S-N curve for CLD construction, where the S-N curve relates to a conventional R-ratio defined as $R = 0.1$ for tension–tension (T-T) loading or $R = -1.0$ for tension–compression (T-C) loading. The methodology distinguishes different fatigue behaviour of CFRP laminates based on their respective ultimate tensile strength (UTS) and ultimate compressive strength (UCS) values, causing the CLD model to consist of two sub-models. The first sub-model, applicable to laminates showing UTS $\geqslant$ |UCS|, is validated for T-T, T-C and compression-compression (C-C) loading by using two carbon-epoxy coupon case studies with lay-ups of $[90/0/90]_{2S}$ and $[45/90/\text{-}45/0]_{2S}$. The second sub-model, applicable to laminates showing |UCS| > UTS, is validated using two carbon-epoxy coupon case studies with laminate lay-ups of $[\pm 60]_{3S}$ and $[45]_{16}$. Agreements between predicted fatigue lives (in the range of interest: $10^3 \leqslant N_f \leq 10^6$) using the proposed CLD method and experimentally obtained fatigue lives are acquired, with prediction errors in similar ranges as those of the original anisomorphic models.

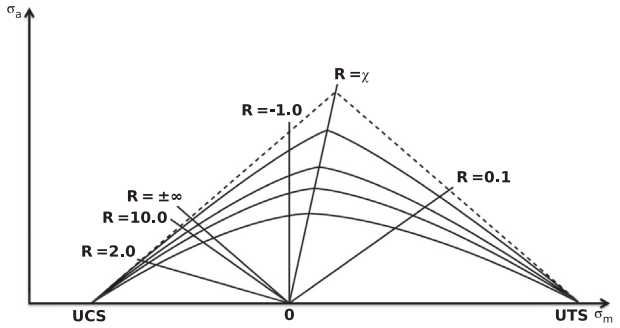

Fig. 1. Proposed CLD model describing the fatigue behaviour of carbon-epoxy laminates characterised by UTS ≥ |UCS|.

2. Methodology

The CLD formulation relies on the relation between mean stress (σ_m), amplitude stress (σ_a) and stress ratio (R), which relate as

$$\sigma_a = \frac{1 - R}{1 + R}\sigma_m. \tag{1}$$

In a CLD, σ_m is plotted on the x-axis and σ_a on the y-axis, as shown in Fig. 1. Different combinations of σ_m and σ_a lead to different R-ratios, related through Eq. (1), of which constant values are described by radial lines arising in the origin. Since each S-N curve also relates to a constant R-ratio, each radial is associated with a particular S-N curve. In the CLD, constant life lines (CLLs) are plotted that each correspond to a constant fatigue life N_f. These CLLs converge to two values on the x-axis: (1) UTS for positive mean stresses and (2) UCS for negative mean stresses. For certain CFRP laminates, both Ansell et al. [1] and Kawai and Koizumi [12] have shown that the peaks of the CLLs are located near the critical R-ratio χ, defined as

$$\chi = \frac{UCS}{UTS}. \tag{2}$$

The boundary of the CLD is given by the x-axis and two linear CLLs corresponding to $N_f = 1$, i.e. static strength, which also peak at the critical R-ratio (σ_m^{χ}, σ_a^{χ}).

The peaks of the CLLs are not located near the critical R-ratio for all CFRP laminates. As seen in results presented by Kawai and Murata [13] and by Kawai and Itoh [11], a disruption in the CLD shape is present for certain angle-ply and off-axis UD laminates. CLLs no longer peak near the critical R-ratio but are shifted towards lower R-ratios, namely towards $R = \pm\infty$: the radial defining the boundary between the T-C and C-C loading region. Moreover, the behaviour of these CFRP laminates under C-C loading indicates higher mean stress sensitivity, and all CLLs intersect the radial for $R = \pm\infty$ in the top region with higher σ_a and σ_m values.

The previous observations concerning the shape of the CLD lead the authors of this work to distinguish between different CFRP laminates based on their UTS and UCS values. This results in the following assumption concerning the CLL peak location:

- For CFRP laminates showing a higher UTS than absolute UCS, i.e. UTS $\geqslant$ |UCS|, the CLLs peak at the critical R-ratio χ.
- For CFRP laminates showing a higher absolute UCS than UTS, i.e. |UCS| > UTS, the CLLs peak at R-ratios in the interval $(-\infty, \chi]$.

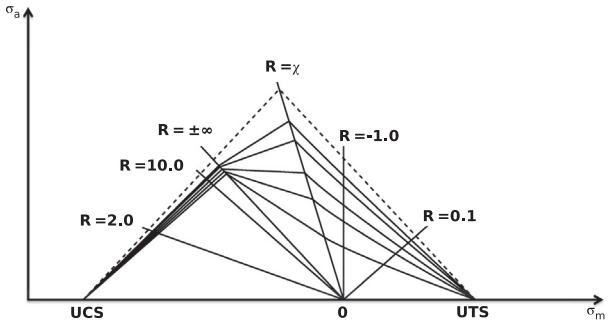

Fig. 2. Proposed CLD model describing the fatigue behaviour of carbon-epoxy laminates characterised by |UCS| > UTS.

In addition, the following assumptions are made for the CLD methodology proposed in this work:

- The CLLs converge to $\sigma_m = UTS$ or $\sigma_m = UCS$ for $\sigma_a = 0$.
- For CFRP laminates characterised by UTS ⩾ |UCS|, the shape of the CLL is a straight line for $N_f = 1$ and converts to a parabola for larger fatigue lives (similar as for the two-segment anisomorphic CLD of Kawai and Koizumi [12]).
- For CFRP laminates characterised by |UCS| > UTS, the shape of the CLLs for an R-ratio in the interval $[\chi, 1.0)$ is a function of χ, while the CLL shape for $R > 1.0$ (C-C type loading) and $R < \chi$ (T-C type loading) is linear.
- For CFRP laminates characterised by |UCS| > UTS, CLLs intersect the $R = \pm\infty$ radial close to $N_f = 1$ due to high mean stress sensitivity under C-C type loading.

Essentially, in this work, two CLD shapes are identified for carbon-epoxy laminates: one applicable to lay-ups characterised by UTS ⩾ |UCS|and one for those by |UCS| > UTS, shown in Figs. 1 and 2, respectively. This distinction is also evident in the presented CLD methodology; two, closely related, CLD models are proposed. The manner of constructing each CLD is discussed next.

2.1. CLD for UTS ⩾ |UCS|

The CLD for carbon-epoxy laminates with a lay-up resulting in UTS ⩾ |UCS|can be divided into two regions: (1) T-T and T-C loads where $1 > R \geqslant \chi$, and (2) T-C and C-C loads where $R < \chi$ or $R > 1.0$. This CLD definition is similar to that presented by Kawai and Koizumi [12], who defined the CLLs as

$$-\frac{\sigma_a - \sigma_a^{\chi}}{\sigma_a^{\chi}} = \begin{cases} \left(\frac{\sigma_m - \sigma_m^{\chi}}{UTS - \sigma_m^{\chi}}\right)^{(2-\psi_{\chi})^z}, & \text{if } \sigma_m^{\chi} \leqslant \sigma_m \leqslant UTS, \\ \left(\frac{\sigma_m - \sigma_m^{\chi}}{UCS - \sigma_m^{\chi}}\right)^{(2-\psi_{\chi})^z}, & \text{if } UCS \leqslant \sigma_m < \sigma_m^{\chi}. \end{cases} \tag{3}$$

In this set of equations, z equals 1.0 and is not part of the original formulation by Kawai and Koizumi [12]. It is introduced in this paper for consistency with the CLD formulation for |UCS| > UTS, as will become clear from the discussion of the second sub-model. The CLD can be constructed by determining the values for σ_a^{χ} and σ_m^{χ}, which can be obtained by performing fatigue life tests under $R = \chi$ as shown by Kawai and Koizumi [12]. However, as previously stated, the critical R-ratio is not conventionally used. Therefore, an adaptation of the anisomorphic CLD is proposed next in order to accommodate the use of fatigue life data obtained under a more conventional R-ratio of either $R = 0.1$ or $R = -1.0$.

Assuming that the CLL formulation (Eq. (3)) as presented by Kawai and Koizumi [12] accurately predicts the fatigue life of carbon-epoxy laminates at $R = 0.1$ and $R = -1.0$ loads, one can infer the validity of a reversed CLL construction procedure that allows for input of fatigue life data obtained at $R = 0.1$ or $R = -1.0$ while providing a similar predictive accuracy. The location of the CLL peak, $(N_f, \sigma_m^{\chi}, \sigma_a^{\chi})$, is no longer known from experimental data; instead, a different input datapoint is given, namely $(N_f, \sigma_m^{I}, \sigma_a^{I})$, which is located on the CLL. Note that if the input datapoints correspond to a constant R-ratio, all data will be located on one radial. Hence, by changing the input R-ratio, the datapoints in the CLD are now related to a radial that no longer corresponds to the critical R-ratio χ. However, for the CLL formulation defined in Eq. (3), not these datapoints, but those related to the CLL peak $(N_f, \sigma_m^{\chi}, \sigma_a^{\chi})$ are required. These can be calculated, provided that the initial assumption regarding the accuracy of the CLL formulation is valid. The set of equations that must be solved to obtain the CLL peak locations at $R = \chi$ is given as

$$\sigma_a^{I} = \begin{cases} \sigma_a^{\chi}\left(1 - \left(\frac{\sigma_m^{I} - \sigma_m^{\chi}}{UTS - \sigma_m^{\chi}}\right)^{(2-\psi_{\chi})^z}\right), & \text{if } \sigma_m^{\chi} \leqslant \sigma_m^{I} \leqslant UTS, \\ \sigma_a^{\chi}\left(1 - \left(\frac{\sigma_m^{I} - \sigma_m^{\chi}}{UCS - \sigma_m^{\chi}}\right)^{(2-\psi_{\chi})^z}\right), & \text{if } UCS \leqslant \sigma_m^{I} < \sigma_m^{\chi}, \end{cases} \tag{4}$$

$$\sigma_a^{\chi} = \sigma_m^{\chi}\frac{1-\chi}{1+\chi}. \tag{5}$$

This set of equations can be solved for σ_m^{χ} and σ_a^{χ}, given that $(N_f, \sigma_m^{I}, \sigma_a^{I})$, UTS, and UCS are known from input data. Moreover, z equals 1.0, and ψ_{χ} is the fatigue strength ratio, which has a definition similar to that given by Kawai and Koizumi [12] as

$$\psi_{\chi} = \frac{\sigma_{\max}^{\chi}}{\sigma_B}. \tag{6}$$

$\sigma_{\max}^{\chi}$ is unknown but can be expressed in terms of the CLL peak stresses as

$$\sigma_{\max}^{\chi} = \begin{cases} \sigma_m^{\chi} + \sigma_a^{\chi}, & \text{if } \sigma_m^{\chi} > 0, \textit{ i. e. } \textit{if } -1 < \chi < 1, \\ \sigma_m^{\chi} - \sigma_a^{\chi}, & \text{if } \sigma_m^{\chi} < 0, \textit{ i. e. } \textit{if } \chi < -1, \\ \sigma_a^{\chi}, & \text{if } \sigma_m^{\chi} = 0, \textit{ i. e. } \textit{if } \chi = -1. \end{cases} \tag{7}$$

Lastly, σ_B is formulated differently than in the definition given by Kawai and Koizumi [12]; in this work, σ_B is no longer derived by means of back-extrapolation from the best curve fit for $R = \chi$, but is instead defined as:

$$\sigma_B = \begin{cases} UTS, & \text{if } UTS > |UCS|, \\ |UCS|, & \text{if } UTS < |UCS|, \\ UTS = |UCS|, & \text{if } UTS = |UCS|. \end{cases} \tag{8}$$

Note that for CFRP laminates characterised by UTS ⩾ |UCS|, as considered for the first sub-model, σ_B always equals UTS.

After solving for $(N_f, \sigma_m^{\chi}, \sigma_a^{\chi})$, an S-N curve equation can be fitted to the obtained datapoints, similar as for the anisomorphic CLD, given by Kawai and Koizumi [12] as

$$N_f = \frac{1}{K_{\chi}}\frac{(1-\psi_{\chi})^a}{\psi_{\chi}^n}, \tag{9}$$

where K_{χ}, a, and n are curve fitting parameters. However, note that any curve fitting function can be employed, and that the CLD method is not bound to the presented equation. In this work, the S-N curve is fitted using a least squares percentage regression (LSPR) [22], which is presumed to be different from Kawai and Koizumi who did not provide details about their fitting method. Note that this difference may cause variations between the fatigue life predictions using the four-segment anisomorphic model as presented in this work (Section 4) and those presented in the work of Kawai and his colleagues.

Subsequently, after fitting Eq. (9) to the predicted CLL peak datapoints for $R = \chi$, Eq. (3) can be used to establish the complete CLD; a procedure similar to that described by Kawai and Koizumi [12]. The methodology presented in this work thus makes it possible to construct the CLD for carbon-epoxy laminates with a lay-up characterised by

UTS ⩾ |UCS|, using only fatigue life data related to either $R = 0.1$ or $R = -1.0$.

2.2. CLD for |UCS| > UTS

For certain angle-ply and off-axis carbon-epoxy laminates, the previously described CLD shape is no longer applicable, as also shown for the anisomorphic model by Kawai and Murata [13] and Kawai and Itoh [11]. These laminates are all are characterised by |UCS| > UTS, an observation used in this work to distinguish between the two CLD models. The CLD in the second sub-model no longer consists of two regions but can instead be divided into three regions, with boundaries at $R = \chi$ and $R = \pm\infty$:

1. $\sigma_m^{\chi} \leqslant \sigma_m \leqslant$ UTS (T-T and T-C loads),
2. $\sigma_m^{-\infty} \leqslant \sigma_m < \sigma_m^{\chi}$ (T-C loads),
3. UCS $\leqslant \sigma_m \leqslant \sigma_m^{\infty}$ (C-C loads),

where $\sigma_m^{\pm\infty}$ is the mean stress on the radial $R = \pm\infty$. The experimental input data used in this work relates to $R = 0.1$ or $R = -1.0$ and is thus always located in the first CLD segment: |UCS| > UTS implies that $\chi < -1.0$.

CLL expressions can be established for each CLD segment, with the CLLs connecting at the boundary radials of $R = \chi$ and $R = \pm\infty$. In this work, the set of CLL functions for a given N_f is defined as:

$$-\frac{\sigma_a - \sigma_a^{\chi}}{\sigma_a^{\chi}} = \left(\frac{\sigma_m - \sigma_m^{\chi}}{UTS - \sigma_m^{\chi}}\right)^{(2-\psi_{\chi})^z} \quad \text{if } \sigma_m^{\chi} \leqslant \sigma_m \leqslant UTS, \tag{10}$$

$$\frac{\sigma_a - \sigma_a^{\chi}}{\sigma_a^{\chi} - \sigma_a^{\pm\infty}} = \frac{\sigma_m - \sigma_m^{\chi}}{\sigma_m^{\chi} - \sigma_m^{\pm\infty}} \quad \text{if } \sigma_m^{-\infty} \leqslant \sigma_m < \sigma_m^{\chi}, \tag{11}$$

$$\frac{\sigma_a - \sigma_a^{\pm\infty}}{\sigma_a^{\pm\infty}} = \frac{\sigma_m - \sigma_m^{\pm\infty}}{\sigma_m^{\pm\infty} - UCS} \quad \text{if } UCS \leqslant \sigma_m \leqslant \sigma_m^{\infty}. \tag{12}$$

In these equations, (σ_m, σ_a) is the varying mean and amplitude stress combination for the considered N_f, while $(\sigma_m^{\chi}, \sigma_a^{\chi})$ and $(\sigma_m^{\pm\infty}, \sigma_a^{\pm\infty})$ are the mean and amplitude stress combination at the intersection of the CLL and the radial for $R = \chi$ and $R = \pm\infty$, respectively. Moreover, note that ψ_{χ} is determined by means of Eq. (6) where, for the laminates considered in this sub-model, $\sigma_B = |\text{UCS}|$.

Eq. (10) is similar to the first CLL definition in the CLD model for UTS ⩾ |UCS|(Eq. (3)). However, z is no longer equal to 1.0. Instead, the exponent z is a function of χ, where

$$z = \begin{cases} 1.0, & \text{if } -1.0 \leqslant \chi < 0.0, \\ \frac{1}{4}(\chi + 1), & \text{if } -\infty \leqslant \chi < -1.0. \end{cases} \tag{13}$$

The exponent z is introduced in this work to describe the observed shape transformation of the CLLs in the first CLD segment as a function of χ. Based on the provided fatigue life results by Kawai and Murata [13] and Kawai and Itoh [11], it can be concluded that for laminates with a lay-up resulting in |UCS|≈UTS, the CLLs have an almost linear shape. However, if χ further decreases, the CLLs approach a convex shape. The proposed inclusion of z in the CLL formulation makes it possible to describe this shape transition. Note that Eq. (13) contains a discontinuity at $R = -1.0$. However, this is deemed acceptable due to large variations seen between the CLD shapes for laminates characterised by UTS ⩾ |UCS|and |UCS| > UTS.

The CLL definition in Eq. (11) is linear and similar to the definitions of the CLLs in the transitional zones defined in the three- and four-segment anisomorphic model of Kawai and Murata [13] and Kawai and Itoh [11], respectively. Yet differences exist related to the definition of the boundary R-ratios, which are, contrarily to the anisomorphic models, fixed at a specific boundary radial. The CLL definition for the third CLD segment (Eq. (12)) is linear due to the high mean stress sensitivity under C-C loading.

Table 1
Static strength test results.

Tensile Static Strength		Compressive Static Strength	
Specimen	Failure Strength [MPa]	Specimen	Failure Strength [MPa]
T-1	662.4	C-1	405.1
T-2	672.5	C-2	402.5
T-3	688.0	C-3	411.5
T-4	715.5	C-4	414.9
		C-5	422.8
		C-6	412.4
Mean Failure Strength	684.6 MPa	Mean Failure Strength	411.5 MPa
Sample Standard Deviation	23.14 MPa	Sample Standard Deviation	7.24 MPa
Coefficient of Variation	3.38%	Coefficient of Variation	1.76%

After establishing the CLL definitions and z-relation, the intersections of the CLLs with the boundary radials must be determined. In this work, experimental data corresponds to either $R = 0.1$ or $R = -1.0$. Therefore, it is first needed to establish the intersection with the radial for $R = \chi$, i.e. $(N_f, \sigma_m^{\chi}, \sigma_a^{\chi})$. In a similar manner as for the first CLD sub-model, $(N_f, \sigma_m^{\chi}, \sigma_a^{\chi})$ can be obtained by solving the set of equations given by Eqs. (4) and (5). However, note that z is now defined by Eq. (13) instead. Next, Eq. (9) can be fitted using LSPR to the obtained values for $(N_f, \sigma_m^{\chi}, \sigma_a^{\chi})$, which results in the predicted S-N curve for $R = \chi$. This S-N curve can be used to construct the CLLs in the first CLD segment, where $\chi \leqslant R < 1.0$. In order to construct the CLLs in the second and third CLD segment, where $R < \chi$ and $R > 1.0$, respectively, it is required to determine the CLL intersections with the second boundary radial related to $R = \pm\infty$. As previously assumed, the CLLs will intersect the $R = \pm\infty$-radial in the top region due to high mean stress sensitivity under C-C loading. The intersection of a CLL for a given N_f with the $R = \pm\infty$-radial can then be described using Eq. (9)

$$\sigma_a^{\pm\infty} = \frac{\frac{1}{10}\sigma_a^{\pm\infty, N_f=1}}{\log_{10}(10^6)}\log_{10}(N_f), \tag{14}$$

where $\sigma_a^{\pm\infty}$ is the amplitude stress at the intersection, and $\sigma_a^{\pm\infty, N_f=1}$ is the amplitude stress describing the intersection between the $R = \pm\infty$-radial and the static strength CLL ($N_f = 1$).

Knowing the intersections of the CLLs with the two boundary radials permits one to construct the complete CLD. The CLL intersections with the radials of $R = \chi$ and $R = \pm\infty$, i.e. $(N_f, \sigma_m^{\chi}, \sigma_a^{\chi})$ and $(N_f, \sigma_m^{\pm\infty}, \sigma_a^{\pm\infty})$, respectively, can be introduced in Eqs. (10)–(12), resulting in a CLL definition for all load ranges. The second methodology presented in this section thus establishes the CLD model for carbon-epoxy laminates with a lay-up characterised by |UCS| > UTS, based solely on fatigue life data related to either $R = 0.1$ or $R = -1.0$.

3. Experimental test set-up and results

Four case studies are considered to assess the predictive performance of the proposed CLD model. To validate the first sub-model, a carbon-epoxy laminate with a lay-up of $[90/0/90]_{2S}$ is used of which the manufacturing and experimental campaign is discussed in this section. Additionally, one case study from literature with a lay-up of $[45/90/-45/0]_{2S}$ is used to evaluate the first sub-model. The validity of the second sub-model is assessed via two case studies from literature with lay-ups of $[\pm 60]_{3S}$ and $[45]_{16}$. These experimental campaigns are not discussed here; instead, the reader is referred to the corresponding papers by Kawai and Koizumi [12], Kawai and Murata [13], and Kawai and Itoh [11], respectively, for details concerning the manufacturing and test procedures.

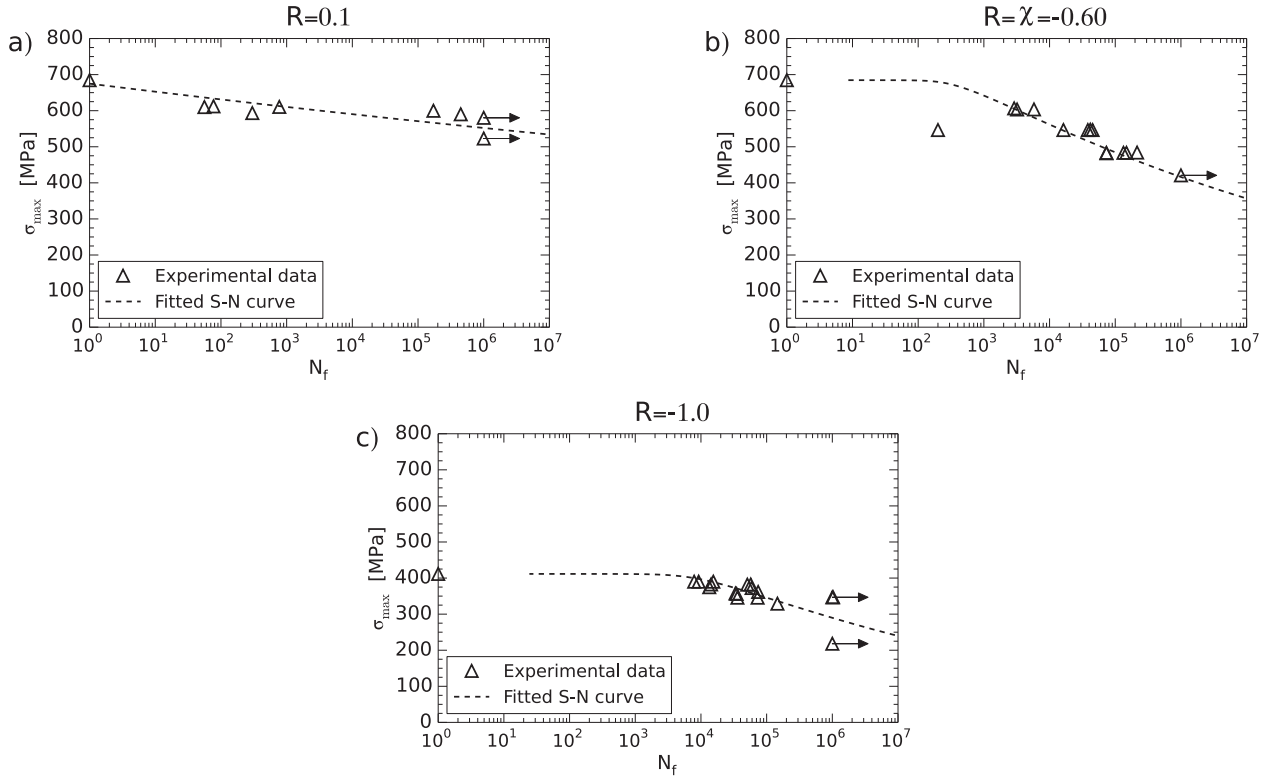

Fig. 3. Experimental fatigue life data for (a) $R = 0.1$, (b) $\chi = -0.60$, and (c) -1.0. Fitted mean S-N curves shown by dashed lines, and run-outs are indicated with an arrow.

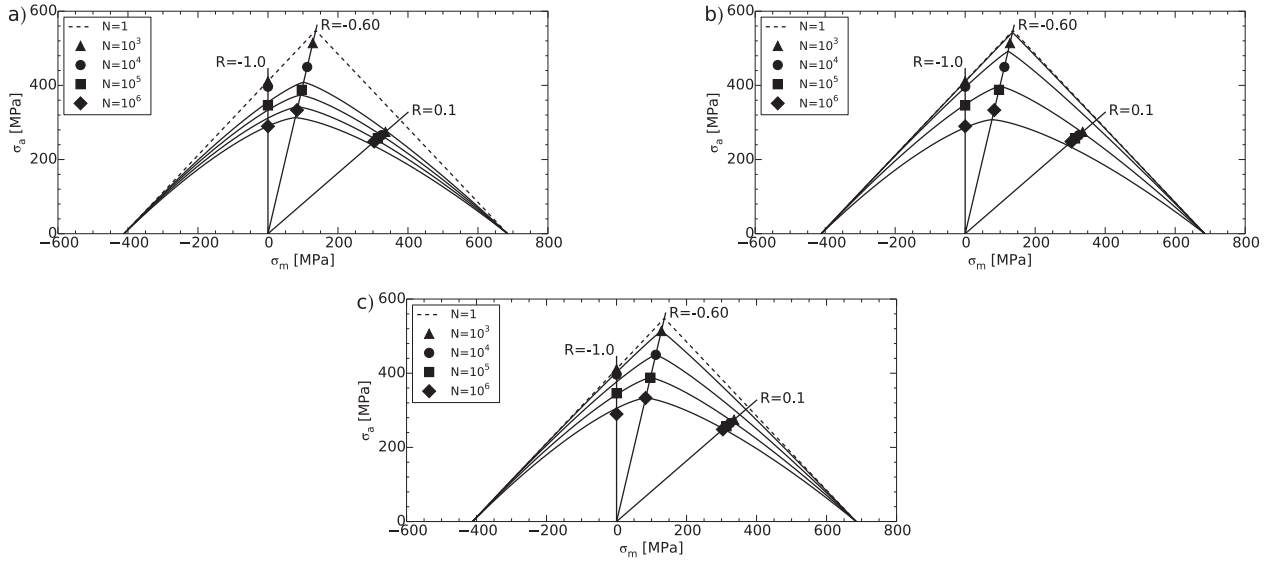

Fig. 4. Constant fatigue life diagram for $[90/0/90]_{2S}$ carbon-epoxy laminate, obtained using the proposed model with (a) $R = 0.1$ and (b) $R = -1.0$ data as input, and (c) using the two-segment anisomorphic model with $R = \chi$ data as input.

A laminate with lay-up of $[90/0/90]_{2S}$ and average thickness of 2.28 mm was manufactured from a Hexcel AS4/8552 carbon-epoxy UD prepreg using hand lay-up, with a debulking procedure performed after every three plies. Next, the laminate was cured in an autoclave following the cycle recommended by the manufacturer [10]. Afterwards, the laminate was roughly cut using a Carat liquid-cooled diamond saw, followed by precise cutting using a Proth Industrial liquid-cooled saw to obtain rectangular specimens. Two specimen geometries were obtained: one for tensile tests, and one for compressive and combined (T-C) tests. The tensile test coupons have a length of 250 mm and width of 25 mm according to ASTM standards D3039/D3039M and D3479/3479M [2,3]. Specimens for the compressive and combined tests are smaller, with a length of 140 mm and width of 12 mm according to ASTM standard D6641/D6641M [4].[1] This smaller size is required in order to reduce the chance of buckling under compressive loads since no anti-buckling device has been used. ASTM standard D6641/D6641M [4]

[1] A newer version of this standard [5]) states a nominal width and gauge length of 13 mm rather than 12 mm. However, the pre-available cutting tool was based on the first version of the standard and due to their small difference of 1 mm, it was decided to follow the first version of the standard instead.

Table 2
Model fitting parameter values for K_χ, a, and n for the $[90/0/90]_{2S}$-laminate. Proposed CLD model: S-N curve fitted to predicted fatigue life datapoints for $R = \chi$ (input of $R = 0.1$ or $R = -1.0$). Two-segment anisomorphic model: S-N curve fitted to experimental fatigue life data for $R = \chi$.

	Proposed Model		Anisomorphic Model
	$R = 0.1$	$R = -1.0$	$R = \chi$
K_χ	2.46	$7.94 \cdot 10^{-5}$	$9.86 \cdot 10^{-4}$
a	$1.00 \cdot 10^{-6}$	0.46	0.34
n	25.70	8.05	14.50

recommends a gauge length of 12 mm to minimise the buckling risk; however, due to test machine limitations, the gauge length was instead 17 mm. Specimens that showed buckling during testing were omitted from the final results. Lastly, thick paper tabs (approximate thickness of 0.15 mm) were glued to the specimens using cyanoacrylate to increase clamping grip.

Both static strength and fatigue life tests were performed using an in-house developed fatigue machine with hydraulic grips. All tests were performed at room temperature with no attempts to control humidity. Static strength tests were displacement-controlled at a nominal rate of 2.0 and 1.3 mm/min (tensile and compressive) according to ASTM standard D3039/D3039M [2]) and D6641/D6641M [5]), respectively. These tests were conducted to acquire the UTS and UCS value, which were determined by averaging the results from four and six specimens, respectively. Table 1 presents the results from the static strength tests, with an average UTS value of 684.6 MPa and an average UCS value of − 411.5 MPa.

CA fatigue tests were performed at three R-ratios, namely $R = 0.1$, $R = -1.0$, and $R = \chi$, where the latter equals − 0.60 based on the average values found for UTS and UCS. These tests were load-controlled and performed at a testing frequency f of 10 Hz. Tests were terminated when reaching one million cycles, after which the specimen is considered a run-out. The experimental fatigue life test results are presented in Fig. 3 for (a) $R = 0.1$, (b) $R = \chi = -0.60$, and (c) $R = -1.0$. For $R = 0.1$, two datapoints obtained under $f = 5$ Hz were included to expand the size of the dataset. In addition, each figure features a mean S-N curve, which was obtained by fitting Eq. (9) to the test results.

The experimental results indicate a large fatigue insensitivity that manifests itself as large scatter in the fatigue lives. This effect was also discussed by Nijssen [17], who stated that, in general, larger fatigue life scatter is seen for flatter S-N curves than for steeper S-N curves. The fatigue sensitivity is lowest for $R = 0.1$, resulting in a nearly linear S-N curve with small slope, while the S-N curve for $R = \chi$ has the largest slope, as well as a low-cycle fatigue plateau. While test results for $R = \chi$ are spread throughout the fatigue life range of interest ($10^3 \leqslant N_f \leq 10^6$), those for $R = -1.0$ are concentrated: test results for $N_f < 10^4$ and $N_f > 10^5$ are scarce. This results in an extrapolation of the S-N curve to these fatigue life ranges, which must be taken into account when assessing the CLD methodology in the next section. Lastly, it is recognised that fewer test results are available for $R = 0.1$ than for $R = \chi$ and $R = -1.0$, which was caused by an unexpected number of discarded test specimens (e.g., due to failure in the clamp region).

4. Fatigue life predictions with CLD methodology

This section evaluates both sub-models proposed in this work by assessing their predictive performance on two case studies each. In addition, the results are compared with that of the anisomorphic models; the first sub-model is compared with the two-segment anisomorphic CLD of Kawai and Koizumi [12], while the second sub-model is compared with the four-segment anisomorphic CLD of Kawai and Itoh [11]. To quantitatively compare the models, four metrics are employed, namely (1) mean average percentage error (MAPE), (2) mean

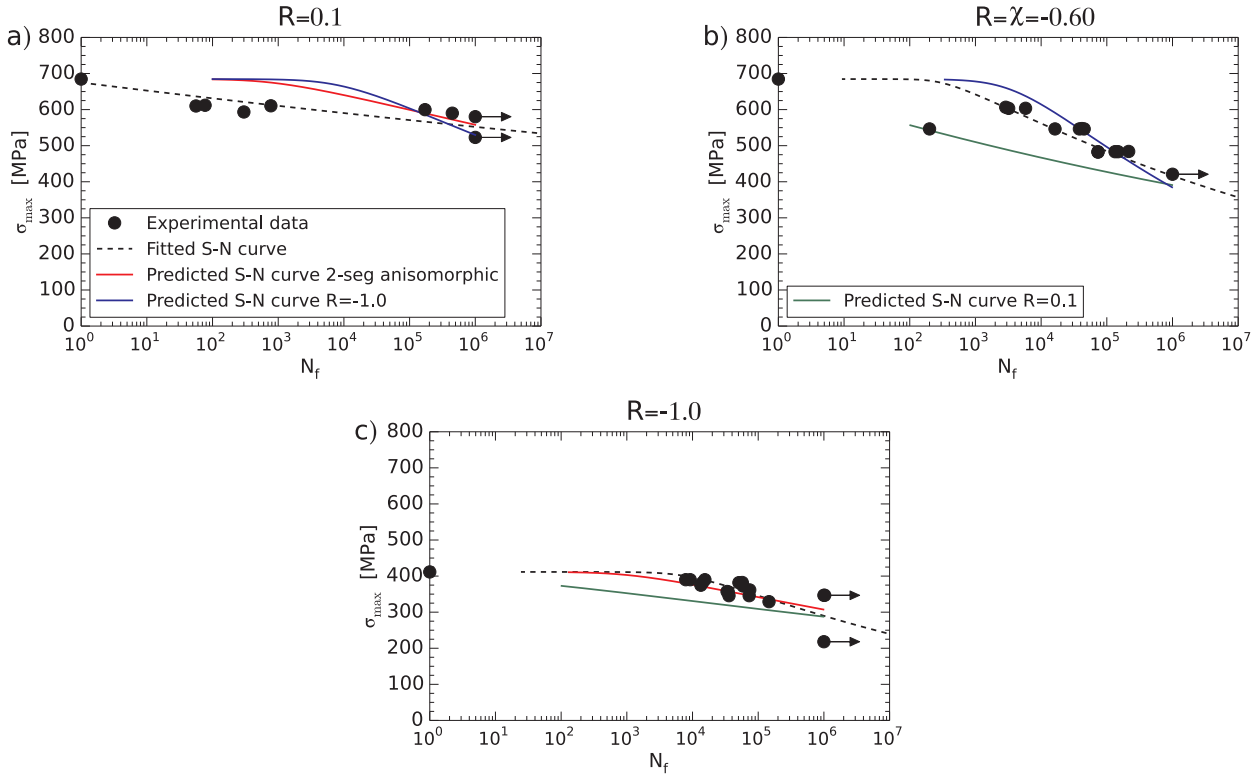

Fig. 5. Fatigue life predictions for $[90/0/90]_{2S}$ of the proposed model (input $R = 0.1$ or $R = -1.0$) and two-segment anisomorphic model (input $R = \chi$). Additionally, experimentally obtained fatigue lives are depicted where run-outs are indicated with an arrow. Fitted and predicted S-N curves are shown for (a) $R = 0.1$, (b) $R = \chi = -0.60$, and (c) $R = -1.0$. Legend is similar for all figures.

Table 3
Metrics for the fatigue life prediction of $[90/0/90]_{2S}$-laminate using the proposed model (input of $R = 0.1$ or $R = -1.0$) and two-segment anisomorphic model (input of $R = \chi$).

Predicted R-ratio	$R = 0.1$		$R = \chi = -0.60$		$R = -1.0$	
	Proposed	Anisomorphic	Proposed		Proposed	Anisomorphic
Input R-ratio	$R = -1.0$	$R = \chi$	$R = 0.1$	$R = -1.0$	$R = 0.1$	$R = \chi$
MAPE [%]	$5.17{\cdot}10^3$	$3.81{\cdot}10^3$	98.00	139.8	98.93	51.64
MNB [%]	$-5.17{\cdot}10^3$	$-3.81{\cdot}10^3$	98.00	−139.8	98.93	49.36
RMSPE [%]	$6.02{\cdot}10^3$	$4.20{\cdot}10^3$	98.02	179.0	98.94	55.71
SSE [%]	86.91	76.97	248.4	10.54	473.8	13.03

Table 4
Model fitting parameter values for K_χ, a, and n for the $[45/90/-45/0]_{2S}$-laminate. Proposed CLD model: S-N curve fitted to predicted fatigue life datapoints for $R = \chi$ (input of $R = 0.1$ or $R = -1.0$). Two-segment anisomorphic model: S-N curve fitted to experimental fatigue life data for $R = \chi$.

	Proposed Model		Anisomorphic Model
	$R = 0.1$	$R = -1.0$	$R = \chi$
K_χ	1.05	$2.47{\cdot}10^{-2}$	$5.62{\cdot}10^{-2}$
a	$1.00{\cdot}10^{-6}$	0.18	0.14
n	13.18	9.03	9.36

normalised bias (MNB), (3) root mean squared percentage error (RMSPE), and (4) sum of squared errors of prediction (SSE). For each metric, a comparison is made between the predicted M_i and true T_i fatigue life. To eliminate influences of single datapoints on the quantitative comparison measures, T_i is defined as the true fatigue life given by the best-fit curve (Eq. (9)))) to the experimental fatigue life datapoints. Note that each metric only provides an indication of the predictive performance of the models with respect to one another; all comparison measures are biased and should only be evaluated simultaneously with S-N curve figures. Regarding the bias, the first three metrics penalise over-prediction more than under-prediction [20] since the percentage values cannot exceed 100% for under-predictions [23]. Therefore, an additional metric, the SSE, is introduced that penalises under-prediction more than over-prediction.

The first metric, MAPE, gives the magnitude of the average percentage relative difference between M_i and T_i, and is defined as

$$\mathrm{MAPE} = \frac{100\%}{n}\sum_{i=1}^{n}\left|\frac{T_i - M_i}{T_i}\right|. \tag{15}$$

MNB assesses the over- or under-prediction of the true fatigue life by the model, and is given as

$$\mathrm{MNB} = \frac{100\%}{n}\sum_{i=1}^{n}\frac{T_i - M_i}{T_i}. \tag{16}$$

The third metric, RMSPE, can be determined as

$$\mathrm{RMSPE} = \sqrt{\frac{1}{n}\sum_{i=1}^{n}\left(\frac{T_i - M_i}{T_i}\cdot 100\%\right)^2}. \tag{17}$$

The last metric, the SSE, is defined as

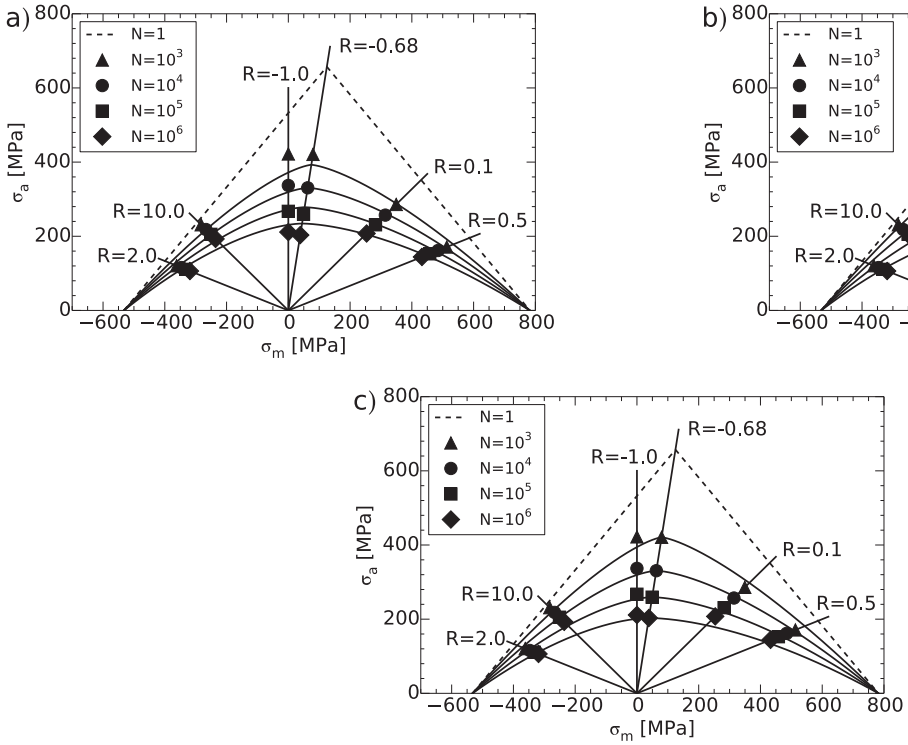

Fig. 6. Constant fatigue life diagram for $[45/90/-45/0]_{2S}$ carbon-epoxy laminate, obtained using the proposed model with (a) $R = 0.1$ and (b) $R = -1.0$ data as input, and (c) using the two-segment anisomorphic model with $R = \chi$ data as input.

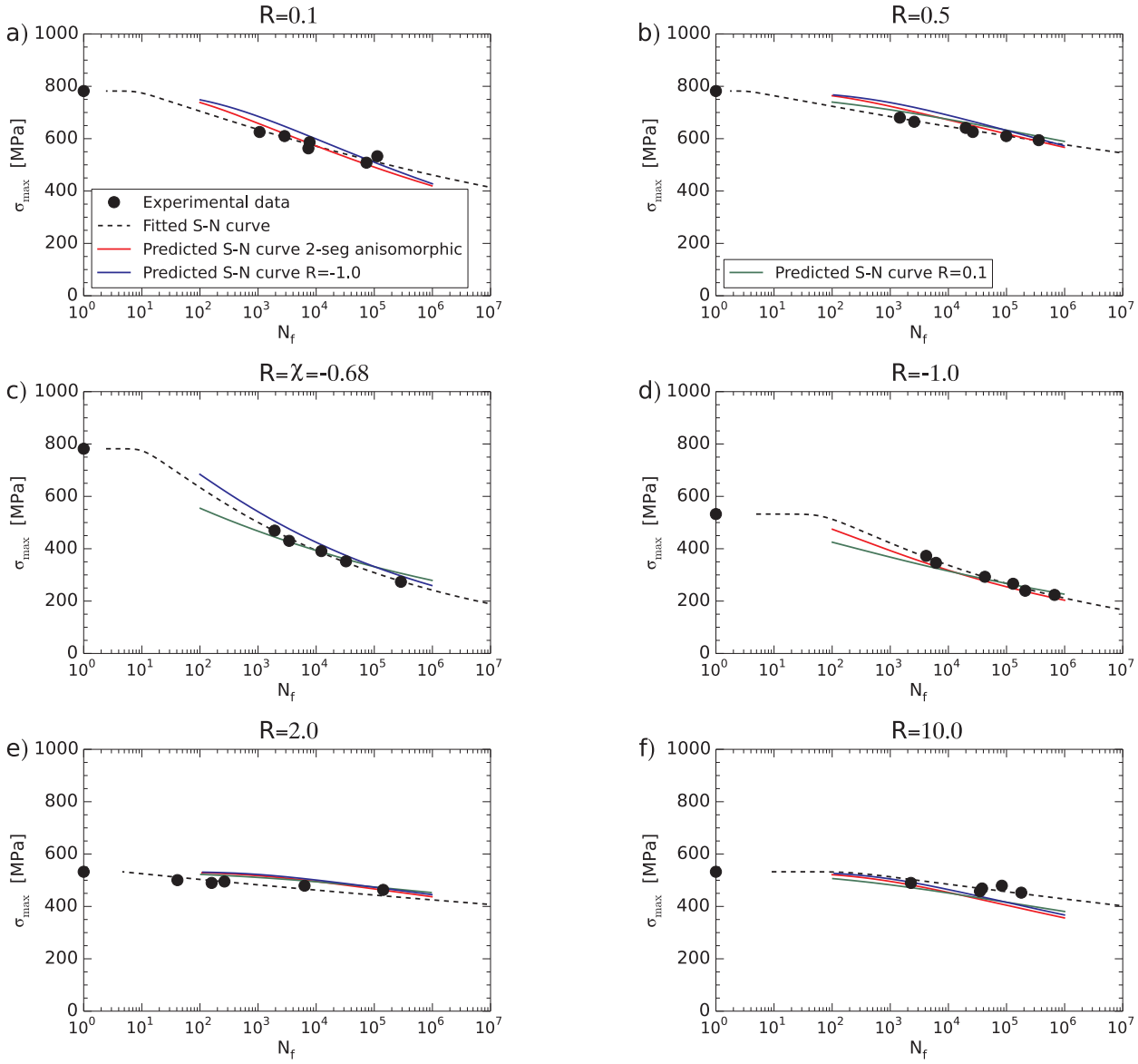

Fig. 7. Fatigue life predictions for $[45/90/-45/0]_{2S}$ of the proposed model (input $R = 0.1$ or $R = -1.0$) and two-segment anisomorphic model (input $R = \chi$). Additionally, experimentally obtained fatigue lives are depicted. Fitted and predicted S-N curves are shown for (a) $R = 0.1$, (b) $R = 0.5$, (c) $R = \chi = -0.68$, (d) $R = -1.0$, (e) $R = 2.0$, and (f) $R = 10.0$. Legend is similar for all figures.

$$\text{SSE} = \sum_{i=1}^{n} (\log(T_i) - \log(M_i)). \tag{18}$$

4.1. $UTS \geqslant |UCS|$

The predictive performance of the first sub-model is assessed using test results obtained during the experimental campaign, discussed in the previous section, and a case study from literature. Both evaluations are discussed next.

4.1.1. $[90/0/90]_{2S}$

Fatigue life data for $R = 0.1$ and $R = -1.0$ was used to predict the fatigue lives for $R = \chi$ and $R = -1.0$, and for $R = 0.1$ and $R = \chi$, respectively. In addition, fatigue life predictions for $R = 0.1$ and $R = -1.0$ were made using the two-segment anisomorphic CLD model of Kawai and Koizumi [12] (with $R = \chi$ as input) to allow for a comparison of the predictive performance of the two models. The CLDs constructed using the model proposed in this work and using the two-segment anisomorphic model are presented in Fig. 4. The models required fitting Eq. (9) to either the experimental or predicted fatigue life datapoints for $R = \chi$ in order to construct the CLDs. This resulted in three sets of fitting parameters, which are presented in Table 2.

Each CLD gives both under- and over-predictions, irrespective of the considered input R-ratio. In order to assess the differences between the models and compare their predictive performances directly, S-N curve predictions have been extracted from each CLD, which are shown in Fig. 5 for (a) $R = 0.1$, (b) $R = \chi = -0.60$, and (c) $R = -1.0$. In addition, each figure displays an S-N curve (Eq. (9)) fitted directly to the experimental test results. The corresponding values for the metrics are included in Table 3. For $R = 0.1$, both the proposed CLD model and the two-segment anisomorphic CLD model show difficulties in accurately predicting the fatigue lives. The experimental data indicates a nearly linear S-N curve with small slope and no distinguishable low-cycle fatigue plateau or fatigue limit. For both $R = \chi$ and $R = -1.0$, a low-cycle fatigue plateau is clearly distinguishable, which results in predicted S-N curves that include a low-cycle fatigue plateau for $R = 0.1$, as shown in Fig. 5a. Consequently, the S-N curve predictions for $R = 0.1$ do not

Table 5
Metrics for the fatigue life prediction of $[45/90/-45/0]_{2S}$-laminate using the proposed model (input of $R = 0.1$ or $R = -1.0$) and two-segment anisomorphic model (input of $R = \chi$).

Predicted R-ratio	$R = 0.1$		$R = 0.5$		$R = \chi = -0.68$		
	Proposed	Anisomorphic	Proposed		Anisomorphic	Proposed	
Input R-ratio	$R = -1.0$	$R = \chi$	$R = 0.1$	$R = -1.0$	$R = \chi$	$R = 0.1$	$R = -1.0$
MAPE [%]	123.3	50.88	308.7	431.6	220.2	89.45	102.3
MNB [%]	−118.2	−25.31	−308.7	−431.6	−214.7	−58.00	−102.3
RMSPE [%]	154.1	59.83	325.2	562.0	300.8	144.2	102.5
SSE [%]	4.19	1.52	11.75	15.29	8.02	2.78	2.48

Predicted R-ratio	$R = -1.0$		$R = 2.0$			$R = 10.0$		
	Proposed	Anisomorphic	Proposed		Anisomorphic	Proposed		Anisomorphic
Input R-ratio	$R = 0.1$	$R = \chi$	$R = 0.1$	$R = -1.0$	$R = \chi$	$R = 0.1$	$R = -1.0$	$R = \chi$
MAPE [%]	56.50	41.19	$3.63{\cdot}10^{3}$	$5.44{\cdot}10^{3}$	$3.24{\cdot}10^{3}$	92.34	75.99	86.34
MNB [%]	2.13	41.19	$-3.63{\cdot}10^{3}$	$-5.44{\cdot}10^{3}$	$-3.24{\cdot}10^{3}$	92.34	75.99	86.34
RMSPE [%]	65.31	41.34	$3.64{\cdot}10^{3}$	$5.75{\cdot}10^{3}$	$3.44{\cdot}10^{3}$	92.34	76.57	86.48
SSE [%]	4.31	1.73	65.46	78.53	59.82	33.09	12.09	21.87

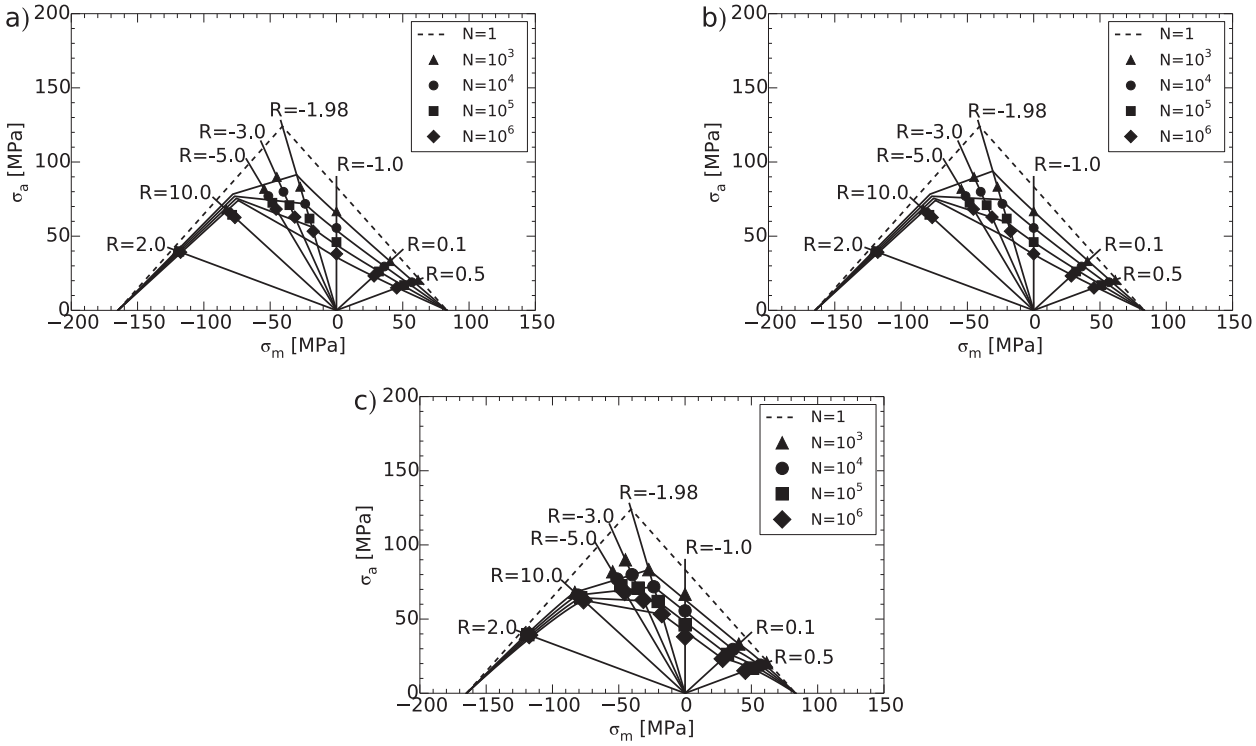

Fig. 8. Constant fatigue life diagram for $[\pm 60]_{3S}$ carbon-epoxy laminate, obtained using the proposed model with (a) $R = 0.1$ and (b) $R = -1.0$ data as input, and (c) using the four-segment anisomorphic model with $R = 0.1$, $R = \chi$, and $R = 10.0$ data as input.

Table 6
Model fitting parameter values for K_χ, a, and n for the $[\pm 60]_{3S}$-laminate. Proposed CLD model: S-N curve fitted to predicted fatigue life datapoints for $R = \chi$ (input of $R = 0.1$ or $R = -1.0$). Four-segment anisomorphic model: S-N curve fitted to experimental fatigue life data for $R = \chi$, $R = 0.1$, and $R = 10.0$.

	Proposed Model		Anisomorphic Model		
	$R = 0.1$	$R = -1.0$	$R = \chi$	$R = 0.1$	$R = 10.0$
K_χ	$1.18{\cdot}10^{-2}$	$1.02{\cdot}10^{-2}$	0.46	$5.12{\cdot}10^{-3}$	1.40
a	0.23	0.24	$4.27{\cdot}10^{-2}$	0.29	$1.00{\cdot}10^{-6}$
n	9.10	9.56	15.43	18.40	83.81

closely describe the fatigue behaviour, irrespective of the chosen CLD model, as confirmed by the metrics in Table 3. The nature of the dataset also affects the fatigue life predictions made using $R = 0.1$ data as input. For lower maximum stress levels under $R = -1.0$, the predictions do approach the experimental results; however, also under-predictions of the fatigue lives are seen for both $R = \chi$ and $R = -1.0$. The applicability of the proposed sub-model becomes more clear from Fig. 5b and c: fatigue life predictions made for $R = \chi$ by means of the proposed model with $R = -1.0$ as input, as well as predictions made for $R = -1.0$ using the two-segment anisomorphic model, show a higher agreement with experimental data. A slight over-prediction by the proposed model can be noted for the lower fatigue life regime $[10^3, 10^4]$ under $R = \chi$; however, one has to take into account that, essentially, an

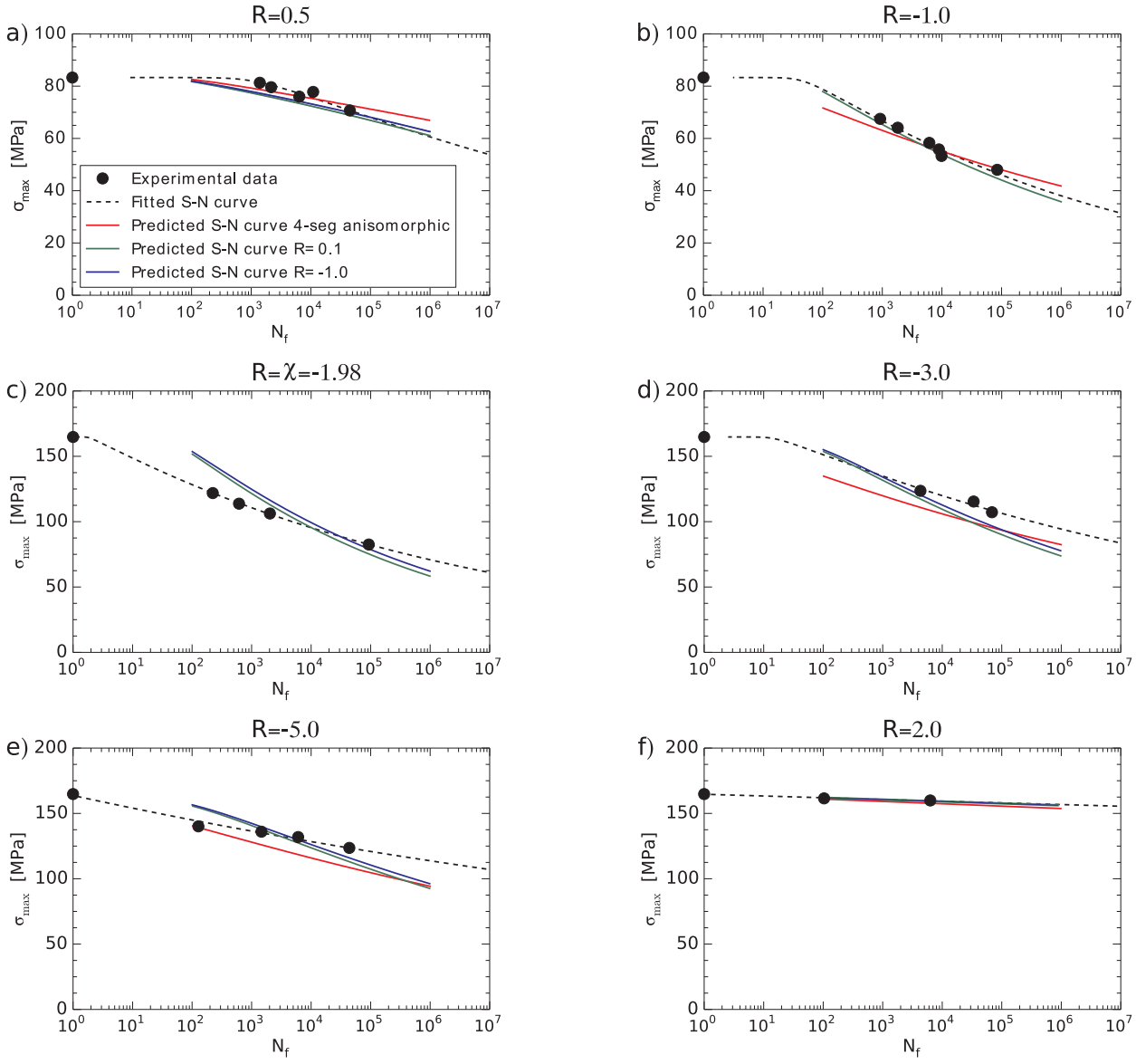

Fig. 9. Fatigue life predictions for $[\pm 60]_{3S}$ of the proposed model (input $R = 0.1$ or $R = -1.0$) and four-segment anisomorphic model (input $R = 0.1$, $R = \chi$, and $R = 10$). Additionally, experimentally obtained fatigue lives are depicted. Fitted and predicted S-N curves are shown for (a) $R = 0.5$, (b) $R = -1.0$, (c) $R = \chi = -1.98$, (d) $R = -3.0$, (e) $R = -5.0$, and (f) $R = 2.0$. Legend is similar for all figures.

extrapolation of the predictions occurs since the original dataset for $R = -1.0$ does not contain data in this lower fatigue life scale. It is expected that when additional input test data in this fatigue life range is included, predictions for $R = \chi$ will improve.

Based on the presented results it can be concluded that, for the $[90/0/90]_{2S}$ laminate, both the two-segment anisomorphic and the proposed model provide a similar predictive accuracy. The predictive accuracy of both models was heavily influenced by the considered experimental dataset, which showed large scatter or did not cover the full fatigue life scale of interest. Yet when taking these aspects into account, the predictions for $R = \chi$ and $R = -1.0$ using $R = -1.0$ and $R = \chi$ as input, respectively, indicate the validity of both the model presented in this work and the anisomorphic model. Moreover, both models face similar issues when predicting the fatigue life for this laminate, thereby touching upon the initial logic of this paper: 'one can infer the validity of a reversed CLL construction procedure that allows for input of fatigue life data obtained at $R = 0.1$ or $R = -1.0$ while providing a similar predictive accuracy' (Section 2). Therefore, even though both models show some difficulties in predicting the fatigue life, these issues are shared and can be attributed to the dataset rather than to the methodology itself. Nevertheless, an additional study case from literature is presented next to attain a stronger basis for the claims made.

4.1.2. $[45/90/-45/0]_{2S}$

A T800H/3631 carbon-epoxy laminate with lay-up of $[45/90/-45/0]_{2S}$, for which experimental data was presented by Kawai and Koizumi [12], is used to evaluate the first sub-model. Experimental data under six R-ratios is available, namely $R = 0.1$, $R = 0.5$, $R = \chi$, $R = -1.0$, $R = 2.0$, and $R = 10.0$. Predictions for $R = 0.5$, $R = 2.0$, $R = 10.0$ can be compared among three curves (one obtained using the two-segment anisomorphic model and two obtained using the proposed model with either $R = 0.1$ or $R = -1.0$ as input), while the other three R-ratios can only be used to compare two S-N curve predictions since these are used as input to one of the considered models. Static strength tests found that UTS and UCS are equal to 781.9 MPa and − 532.4 MPa, respectively, resulting in a critical R-ratio of $\chi = -0.68$.

To construct the CLD using the model proposed in this work, Eq. (9)

Table 7
Metrics for the fatigue life prediction of $[\pm 60]_{3S}$-laminate using the proposed model (input of $R = 0.1$ or $R = -1.0$) and four-segment anisomorphic model (input of $R = 0.1$, $R = \chi$, and $R = 10.0$).

Predicted R-ratio	$R = 0.5$			$R = -3.0$			$R = -5.0$		
	Proposed		Anisomorphic	Proposed		Anisomorphic	Proposed		Anisomorphic
Input R-ratio	$R = 0.1$	$R = -1.0$	$R = 0.1, \chi, 10.0$	$R = 0.1$	$R = -1.0$	$R = 0.1, \chi, 10.0$	$R = 0.1$	$R = -1.0$	$R = 0.1, \chi, 10.0$
MAPE [%]	79.61	71.70	83.76	73.04	62.59	90.32	87.46	122.0	82.82
MNB [%]	79.61	71.70	9.59	73.04	62.59	90.32	−44.83	−88.87	−82.82
RMSPE [%]	80.56	74.38	99.69	73.81	64.03	90.32	−111.0	156.0	83.30
SSE [%]	16.99	12.89	6.18	6.32	3.74	16.36	3.54	3.62	16.64
Predicted R-ratio	$R = -1.0$			$R = \chi = -1.98$			$R = 2.0$		
Input R-ratio	Proposed $R = 0.1$		Anisomorphic $R = 0.1, \chi, 10.0$	Proposed $R = 0.1$			Proposed $R = 0.1$	$R = -1.0$	Anisomorphic $R = 0.1, \chi, 10.0$
MAPE [%]	29.19		39.49	170.0		242.8	10.90	10.76	83.91
MNB [%]	29.19		15.88	−141.0		−225.8	10.48	10.48	83.91
RMSPE [%]	29.70		46.36	201.2		291.2	15.11	15.02	84.09
SSE [%]	0.76		2.17	4.51		6.09	$5.78 \cdot 10^{-2}$	$5.70 \cdot 10^{-2}$	7.39

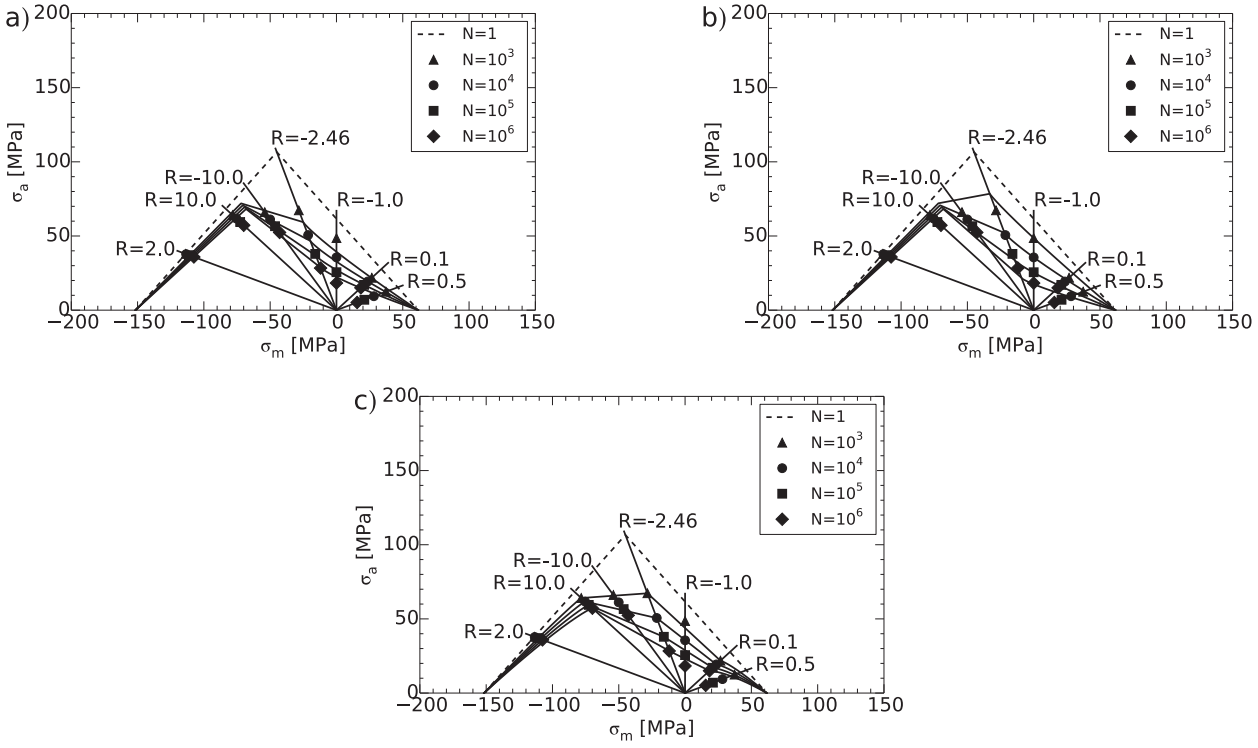

Fig. 10. Constant fatigue life diagram for $[45]_{16}$ carbon-epoxy laminate, obtained using the proposed model with (a) $R = 0.1$ and (b) $R = -1.0$ data as input, and (c) using the four-segment anisomorphic model with $R = 0.1$, $R = \chi$, and $R = 10.0$ data as input.

Table 8
Model fitting parameter values for K_χ, a, and n for the $[45]_{16}$-laminate. Proposed CLD model: S-N curve fitted to predicted fatigue life datapoints for $R = \chi$ (input of $R = 0.1$ or $R = -1.0$). Four-segment anisomorphic model: S-N curve fitted to experimental fatigue life data for $R = \chi$, $R = 0.1$, and $R = 10.0$.

	Proposed Model		Anisomorphic Model		
	$R = 0.1$	$R = -1.0$	$R = \chi$	$R = 0.1$	$R = 10.0$
K_χ	0.25	$2.97 \cdot 10^{-3}$	$3.07 \cdot 10^{-2}$	$6.14 \cdot 10^{-2}$	$2.39 \cdot 10^{-2}$
a	$7.35 \cdot 10^{-2}$	0.35	0.19	0.16	0.20
n	9.54	5.06	7.85	18.25	59.29

needed to be fitted to the fatigue life predictions for $R = \chi$. The fitting parameters are presented in Table 4, together with the direct fitting of Eq. (9) to the experimental datapoints for $R = \chi$; the latter of which is needed for the two-segment anisomorphic CLD. The constructed CLDs are shown in Fig. 6, while the predicted S-N curves and metric values are presented in Fig. 7 and Table 5, respectively. Slight differences are seen in the fatigue life predictions, with larger variations seen for fatigue lives in lower ranges ($[10^3, 10^4]$). Yet all predicted S-N curves are in the vicinity of the experimental data and lie in the same order of magnitude. Moreover, no major differences are seen between the models, and it can be concluded that the proposed CLD model provides a similar predictive performance as the two-segment anisomorphic model.

Table 9
Metrics for the fatigue life prediction of $[45]_{16}$-laminate using the proposed model (input of $R = 0.1$ or $R = -1.0$) and four-segment anisomorphic model (input of $R = 0.1$, $R = \chi$, and $R = 10.0$).

Predicted R-ratio	$R = 0.5$			$R = -1.0$		$R = 2.0$		
	Proposed		Anisomorphic	Proposed	Anisomorphic	Proposed		Anisomorphic
Input R-ratio	$R = 0.1$	$R = -1.0$	$R = 0.1, \chi, 10.0$	$R = 0.1$	$R = 0.1, \chi, 10.0$	$R = 0.1$	$R = -1.0$	$R = 0.1, \chi, 10.0$
MAPE [%]	657.4	$2.07{\cdot}10^3$	$7.77{\cdot}10^3$	80.34	33.86	99.72	99.72	99.50
MNB [%]	−657.4	$-2.07{\cdot}10^3$	$-7.77{\cdot}10^3$	80.34	33.86	99.72	99.72	99.50
RMSPE [%]	664.7	$2.42{\cdot}10^3$	$8.91{\cdot}10^3$	81.01	43.15	99.72	99.72	99.50
SSE [%]	12.25	25.84	54.22	10.85	1.37	88.62	88.93	58.94
Predicted R-ratio	$R = -10.0$			$R = \chi = -2.46$		$R = 10.0$		
	Proposed		Anisomorphic	Proposed		Proposed		
Input R-ratio	$R = 0.1$	$R = -1.0$	$R = 0.1, \chi, 10.0$	$R = 0.1$	$R = -1.0$	$R = 0.1$		$R = -1.0$
MAPE [%]	38.98	248.3	59.86	42.26	59.21	$7.62{\cdot}10^3$		$7.61{\cdot}10^3$
MNB [%]	−15.05	−230.5	46.28	37.89	−7.66	$-7.57{\cdot}10^3$		$-7.56{\cdot}10^3$
RMSPE [%]	50.72	366.4	63.47	46.33	74.45	$1.25{\cdot}10^4$		$1.25{\cdot}10^4$
SSE [%]	0.99	7.45	8.17	3.99	4.10	37.54		37.61

4.2. $|UCS| > UTS$

The predictive performance of the second sub-model is evaluated using two carbon-epoxy laminates with lay-ups of $[\pm 60]_{3S}$ and $[45]_{16}$ for which experimental datasets were found in literature ([13,11]). Details concerning the manufacturing and testing of the panels can be found in the corresponding papers. In this section, for both lay-ups, a comparison is made with the four-segment anisomorphic model (with k_T and k_C assumed as $k_T = k_C = 1$) proposed by Kawai and Itoh [11]. In contrast to the two-segment anisomorphic model, the four-segment anisomorphic model requires fatigue life data under three R-ratios as input, namely $R = 0.1$, $R = \chi$, and $R = 10.0$; an aspect that should be considered during the comparison. For details concerning the unsuitability of the two-segment anisomorphic model for these case studies and the methodology of the four-segment anisomorphic model, the reader is referred to Kawai and Murata [13] and Kawai and Itoh [11].

4.2.1. $[\pm 60]_{3S}$

For the $[\pm 60]_{3S}$-laminate, fatigue life test results are available under two T-T conditions ($R = 0.1$ and $R = 0.5$), four T-C conditions ($R = -1.0$, $R = \chi = -1.98$, $R = -3.0$, and $R = -5.0$), and two C-C conditions ($R = 2.0$ and $R = 10.0$), with UTS and UCS values equal to 83.3 MPa and − 164.8 MPa, respectively. The CLDs constructed using the model proposed in this work and the four-segment anisomorphic model are presented in Fig. 8. The model proposed in this work requires fitting of Eq. (9) to the predicted fatigue lives for $R = \chi$, for which the corresponding fitting parameters are included in Table 6. For the four-segment anisomorphic model, Eq. (9) was fitted directly to experimental data related to $R = \chi$, $R = 0.1$, and $R = 10.0$, for which the fitting parameters are also shown in Table 6.

The presented CLDs display several similarities. All three diagrams show fatigue life predictions for $\chi < R < 1.0$ and $R > 1.0$ in similar scales as the experimental data, though for $R = \chi$, $R = 10.0$ a distinguishable difference between the models can be seen. Whereas the 4-segment anisomorphic model shows a high accuracy, the proposed models show over- and under-predictions. Note that this difference is caused by the set-up of the models: these R-ratios are used as input to the four-segment anisomorphic model, whereas the fatigue lives for these R-ratios need to be predicted in the proposed model. For $R \leqslant \chi$, predictions using the proposed model (both $R = 0.1$ and $R = -1.0$ as input) are still in the vicinity of the experimental datapoints, but slight over- and under-predictions are seen for lower and higher fatigue lives, respectively, while the four-segment CLD only shows under-predictions for these R-ratios. This becomes more evident when evaluating the predicted S-N curves that are presented in Fig. 9 for (a) $R = 0.5$, (b) $R = -1.0$, (c) $R = \chi = -1.98$, (d) $R = -3.0$, (e) $R = -5.0$, and (f) $R = 2.0$. Note that each figure also features an S-N curve fitted directly to the experimental data (Eq. (9)). In addition, metric values for each model are presented in Table 7.

Analysing Fig. 9, the similarities between the fatigue life predictions using either $R = 0.1$ or $R = -1.0$ as input to the proposed model are apparent. Moreover, the predicted S-N curves are adjacent to the S-N curves fitted directly to the experimental datapoints. This is also true for the four-segment anisomorphic model when predicting $R = 0.5$: differences between the models are minimal. However, when using the four-segment anisomorphic CLD to predict $R = -3.0$, $R = -5.0$ or $R = 2.0$, larger differences are seen with the proposed model, as well as with the best-fit S-N curve. For example, for $R = -3.0$, the predicted S-N curve is parallel to the best-fit S-N curve but results in larger predictive errors. The first three metrics (MAPE, MNB, and RMSPE), as included in Table 7, indicate similar magnitudes of the comparison metrics for all predicted S-N curves. However, one should be aware that this is caused by an under-prediction of the fatigue lives by the four-segment anisomorphic model; the three metrics penalise over-predictions more than under-predictions. When evaluating the fourth metric, the SSE, larger differences are seen between the models because the SSE penalises under-predictions more than over-predictions. Based on both the metrics and the presented CLD and S-N curves, it can be concluded that the proposed CLD sub-model for lay-ups showing |UCS| > UTS predicts the fatigue lives of the carbon-epoxy laminate with lay-up $[\pm 60]_{3S}$ with a similar or higher accuracy than the four-segment anisomorphic CLD model by Kawai and Itoh [11].

4.2.2. $[45]_{16}$

For the $[45]_{16}$-laminate, fatigue life test results are available for $R = 0.1$, $R = 0.5$, $R = -1.0$, $R = \chi = -2.46$, $R = -10.0$, $R = 2.0$, and $R = 10.0$. Static strength tests indicated values of 61.6 MPa and − 151.6 MPa for UTS and UCS, respectively. Both $R = 0.1$ and $R = -1.0$ were used as input to the proposed model and the constructed CLDs are included in Fig. 10a and b, respectively. Table 8 presents the fitting parameters of Eq. (9) to the predicted fatigue lives for $R = \chi$. In addition, the four-segment anisomorphic model was used to construct the CLD, which is shown in Fig. 10c, and its fitting parameters for the experimental data are included in Table 8. To aid in the comparison, values of the four metrics are shown in Table 9 for each model.

The CLDs in Fig. 10 show consistency, independent of the chosen

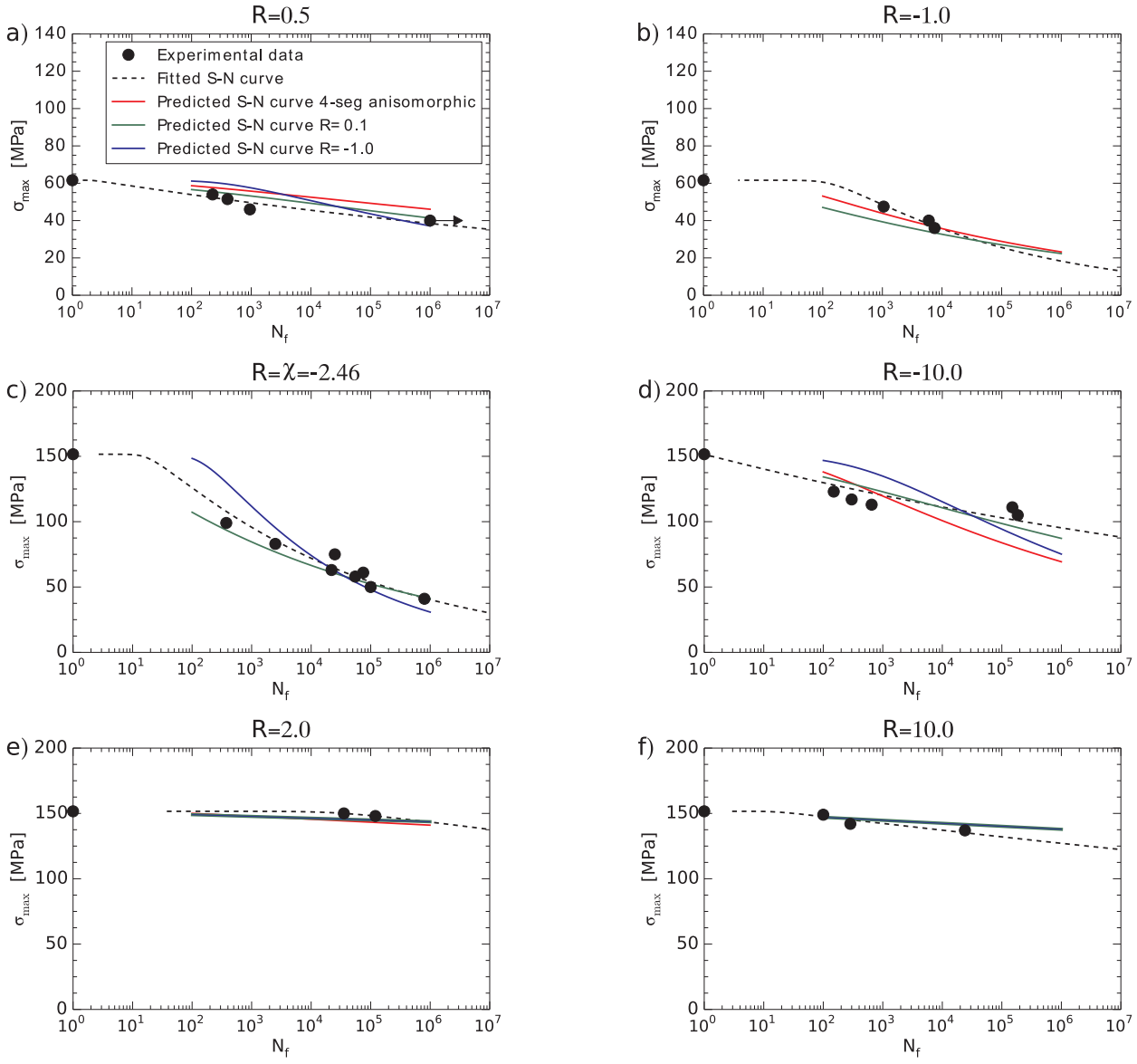

Fig. 11. Fatigue life predictions for $[45]_{16}$ of the proposed model (input $R = 0.1$ or $R = -1.0$) and four-segment anisomorphic model (input $R = 0.1$, $R = \chi$, and $R = 10$). Additionally, experimentally obtained fatigue lives are depicted where run-outs are indicated with an arrow. Fitted and predicted S-N curves are shown for (a) $R = 0.5$, (b) $R = -1.0$, (c) $R = \chi = -2.46$, (d) $R = -10.0$, (e) $R = 2.0$, and (f) $R = 10.0$. Legend is similar for all figures.

model. Moreover, they resemble the trend of the fatigue life test data. Yet a difference is again seen in the prediction of fatigue lives under $R = \chi$ and $R = 10$, which is caused by the difference in input R-ratio to the models, as previously discussed in the case study for $[\pm 60]_{3S}$. Additionally, a contrast is seen in the CLLs corresponding to $N_f = 10^3$, which show differences dependent on the selected model. This also becomes clear from Fig. 11, where the predicted S-N curves, as well as the best-fit curve to the experimental data, are presented. Note that, due to differences in the input R-ratios, comparisons among three predicted S-N curves (one obtained using the four-segment anisomorphic model and two obtained using the proposed sub-model) can only be made for three R-ratios, namely $R = 0.5$, $R = -10.0$, and $R = 2.0$, while the other three R-ratios can only be used to compare two curves.

Predictions for $R = 0.5$, as shown in Fig. 11a, are similar: all models result in over-predictions of the fatigue life. The predicted S-N curves by the proposed model using $R = 0.1$ as input and the four-segment anisomorphic model are almost parallel to the best-fit S-N curve, while the S-N curve predicted using the $R = -1.0$ fatigue life data as input shows a steeper slope. As confirmed by the metric values in Table 9, the proposed model using $R = 0.1$ as input results in an S-N curve closest to the best-fit curve. Fig. 11b and c show the predictions for $R = -1.0$ and $R = \chi$ in which the differences between the models is also small. Moreover, the predicted S-N curves are located close to the best-fit S-N curve.

For $R = -10.0$ the predicted S-N curves show larger differences. The S-N curve predicted using the proposed model with $R = 0.1$ as input is located in the vicinity of the best-fit curve and is nearly linear, but shows a slightly larger slope than the best-fit curve. As also indicated by the metric values in Table 9, this model results in the best predictive performance among all three CLDs. Both the proposed model with $R = -1.0$ as input and the four-segment anisomorphic model show larger slopes and hint at a low-cycle fatigue plateau; the existence of the latter cannot be confirmed by the experimental data. Lastly, Fig. 11e and f show the predictions for the C-C cases ($R = 2.0$ and $R = 10.0$, respectively) with minimal differences between the models, as confirmed by the metric values in Table 9. Overall it can be said that for the maximum stress levels of the test data, all models provide fatigue life predictions in similar ranges as indicated by the experimental

datapoints.

5. Conclusion

A new CLD model was proposed to predict the fatigue life of carbon fibre-reinforced epoxy laminates under CA T-T, T-C, and C-C loading using a single experimental S-N curve related to either $R = 0.1$ or $R = -1.0$. The proposed methodology reduces the size of the input dataset with respect to other CLD methods (e.g., those of Boerstra [6], Gathercole et al. [9], or Vassilopoulos et al. [26]), and employs a more conventional R-ratio than the anisomorphic CLD model of Kawai and Koizumi [12]. To assess variations in mean stress sensitivity for different laminates, the proposed CLD definition was divided into two sub-models: one for laminates characterised by $UTS \geqslant |UCS|$and one for those displaying the opposite tendency, i.e. $|UCS| > UTS$.

The first sub-model demonstrated that a similar CLL definition to that used in the two-segment anisomorphic CLD [12] can be employed to construct the CLD. However, the CLLs were derived using a more conventional R-ratio of $R = 0.1$ or $R = -1.0$ rather than $R = \chi$. This was shown using experimental fatigue life data of an AS4/8552 carbon-epoxy laminate with a $[90/0/90]_{2S}$ lay-up. Due to the nature of the experimental data, which showed large fatigue insensitivity resulting in scatter as well as the concentration of datapoints in certain fatigue life scales, the similarities between the models were not always evident. To strengthen the claim made in this study, an additional study case was presented by considering a T800H/3631 carbon-epoxy laminate with lay-up of $[45/90/-45/0]_{2S}$ from literature. Agreements between the predictive performance of the presented sub-model and the anisomorphic model were shown, thereby providing a stronger basis for the proposal of the second sub-model in this study.

The second sub-model was validated by comparing fatigue life predictions with experimentally obtained data from literature for two case studies: one carbon-epoxy laminate with a lay-up of $[\pm 60]_{3S}$ (T800H/2500) and one with a lay-up of $[45]_{16}$ (T700S/2592). For the considered load cases, it was shown that the predictions in the fatigue life range of interest ($10^3 \leqslant N_f \leq 10^6$) are in the vicinity of the experimental data. The predictions for C-C type loads show minimal differences between the models. This is likely caused by the observation of larger scatter seen in fatigue lives under this type of CA loading due to a higher mean stress sensitivity. Yet predictions are within an acceptable range of the experimental datapoints, and similar or improved predictive performance was seen when compared to the four-segment anisomorphic model proposed by Kawai and Itoh [11].

Though this paper has shown that acceptable predictions are obtained for the considered laminates, it is recommended to further evaluate the applicability of the proposed method to other lay-ups or different composite materials. In addition, the transformation of the CLD shape with respect to the value of χ should be studied in order to strengthen the validity of the assumptions made. Lastly, a final note should be made on the flexibility that the presented model introduces. This study evaluated the proposed CLD model by focusing on the input of a single S-N curve corresponding to a conventional R-ratio of either $R = 0.1$ or $R = -1.0$. However, the setup of the model is such that it allows for input data related to any R-ratio. The steps for CLD construction will be similar even though the location of the input datapoints will differ. Potentially, the CLD model even allows for the input of sparse datapoints: using these to determine the stresses at the segment boundary radial(s), followed by a curve fitting function, permits constructing the full CLD. Hence, the model proposed in this study, by requiring only one S-N curve as input, could reduce the size of the experimental test dataset necessary for fatigue life predictions, thereby reducing expenses in terms of both cost and time.

Declarations of Interest

None.

Funding

This research did not receive any specific grant from funding agencies in the public, commercial, or not-for-profit sectors.

References

[1] Ansell MP, Bond IP, Bonfield PW. Constant life diagrams for wood composites and polymer matrix composites. Proc. of the 9th international conference on composite materials V. 1993. p. 692–9.
[2] ASTM. Standard test method for tensile properties of polymer matrix composite materials. Standard. West Conshohocken, PA, USA: ASTM International; 1971 (2017).
[3] ASTM. Standard test method for tension-tension fatigue of polymer matrix composite materials. Standard. West Conshohocken, PA, USA: ASTM International; 1976 (2012).
[4] ASTM. Standard test method for determining compressive properties of polymer matrix composite laminates using a combined loading compression (CLC) test fixture. Standard. West Conshohocken, PA, USA: ASTM International; 2001.
[5] ASTM. Standard test method for compressive properties of polymer matrix composite materials using a combined loading compression (CLC) test fixture. Standard. West Conshohocken, PA, USA: ASTM International; 2001. (2016).
[6] Boerstra GK. The multislope model: A new description for the fatigue strength of glass fibre reinforced plastic. Int J Fatigue 2007;29:1571–6.
[7] Ellyin F, El-Kadi H. A fatigue failure criterion for fiber reinforced composite laminae. Compos Struct 1990;15:61–74.
[8] Epaarachchi JA, Clausen PD. An empirical model for fatigue behavior prediction of glass fibre-reinforced plastic composites for various stress ratios and test frequencies. Compos Part A: Appl Sci Manuf 2003;34:313–26.
[9] Gathercole N, Reiter H, Adam T, Harris B. Life prediction for fatigue of T800/5245 carbon-fibre composites: I. Constant-amplitude loading. Int J Fatigue 1994;16:523–32.
[10] Hexcel. HexPly 8552 epoxy matrix product datasheet. Hexcel; 2016 [Accessed December 11, 2017].
[11] Kawai M, Itoh N. A failure-mode based anisomorphic constant life diagram for a unidirectional carbon/epoxy laminate under off-axis fatigue loading at room temperature. J Compos Mater 2014;48:571–92.
[12] Kawai M, Koizumi M. Nonlinear constant fatigue life diagrams for carbon/epoxy laminates at room temperature. Compos Part A: Appl Sci Manuf 2007;38:2342–53.
[13] Kawai M, Murata T. A three-segment anisomorphic constant life diagram for the fatigue of symmetric angle-ply carbon/epoxy laminates at room temperature. Compos Part A: Appl Sci Manuf 2010;41:1498–510.
[14] Kohout J, Věchet S. A new function for fatigue curves characterization and its multiple merits. Int J Fatigue 2001;23:175–83.
[15] Mandell JF, Samborsky DD. SNL/DOE/MSU Composite Materials Fatigue Database. https://energy.sandia.gov/energy/renewable-energy/water-power/technology-development/advanced-materials/mhk-materials-database/. Version 25.0; 2015.
[16] Nijssen RPL. "OptiDat Database, Knowledge Centre WMC. http://www.wmc.eu/optimatblades_optidat.php; 2006 [Accessed August 28, 2017].
[17] Nijssen RPL. Fatigue life prediction of composites and composite structures. In: Vassilopoulos AP, editor. Phenomenological fatigue analysis and life modelling. Woodhead Publishing Limited; 2010. p. 47–78.
[18] Passipoularidis VA, Philippidis TP, Brondsted P. Fatigue life prediction in composites using progressive damage modelling under block and spectrum loading. Int J Fatigue 2011;33:132–44.
[19] Samareh-Mousavi SS, Mandegarian S, Taheri-Behrooz F. A nonlinear FE analysis to model progressive fatigue damage of cross-ply laminates under pin-loaded conditions. Int J Fatigue 2019;119:290–301.
[20] Shcherbakov MV, Brebels A, Shcherbakova NL, Tyukov AP, Janovsky TA, Kamaev VA. A survey of forecast error measures. World Appl Sci J 2013;24:171–6.
[21] Shokrieh MM, Taheri-Behrooz F. A unified fatigue life model based on energy method. Compos Struct 2006;75:444–50.
[22] Tofallis C. Least squares percentage regression. J Modern Appl Stat Methods 2008;7:526–34.
[23] Tofallis C. A better measure of relative prediction accuracy for model selection and model estimation. J Operat Res Soc 2015;66:1352–62.
[24] Varvani-Farahani A, Haftchenari H, Panbechi M. An energy-based fatigue damage parameter for off-axis unidirectional frp composites. Compos Struct 2007;79:381–9.
[25] Vassilopoulos AP, Manshadi BD, Keller T. Influence of the constant life diagram formulation on the fatigue life prediction of composite materials. Int J Fatigue 2010;32:659–69.
[26] Vassilopoulos AP, Manshadi BD, Keller T. Piecewise non-linear constant life diagram formulation for FRP composite materials. Int J Fatigue 2010;32:1731–8.